Fabrication of a PLDC Cell using Near Infrared OLED

Vijendra V

Abstract— The fabrication of a single-layer NIR OLED by a new luminescent material. Demonstrate vertically stacked device consisting of organic photovoltaic device (OPV) and organic light-emitting diode (OLED) inside a polymer dispersed liquid crystal (PDLC) cell. In such a device, OLED and PDLC acted as transmissive (T-) and reflective (R-) mode respectively, of a transflective display without the tradeoff of aperture ratio between R- and T- modes in a conventional transflective LC display. The characteristics of this diode is considered and investigated with different thicknesses. Electroluminescence is observed with the peak at 800 nm. Storage lifetime of OLED increased in the stacked device because LC material helped to prevent the water and oxygen attack. Driving voltage of PDLC increased due to the insertion of passivation layer upon the electrode which was used protect the OLED and OPV underneath.

Index Terms— DVS, HOMO, low power design, LUMO, OPV, OLED, PLDC

I. INTRODUCTION

In recent years, OLEDs are being considered for full-color flat-panel displays technology ever since the initial work by Tang and VanSlyke [1]. Organic light-emitting diode (OLED) is one of the emerging display technologies, especially for handheld mobile displays [1]–[3]. However, contrast ratio (CR) of such a display decreases with increasing the ambient light intensity. In display technologies also organic light emitting diodes show great promise with low cost, small size and flexible flat screens[2],[3] with better resolution and wider viewing angles[4]. No need for backlight, also better resolution, higher brightness and low power consumption are other important advantages with respect to liquid crystals display [1].Organic light-emitting diodes (OLEDs) in the visible spectrum region have achieved significant progress since 1987[1]. Near-infrared (NIR) and infrared(IR) OLEDs have also received growing attention because of their applications in information processing[5] and night-vision readable displays[6].So far the IR and NIR organic light-emitting material that have been reported include organic ionic dyes, organic molecules, organic rare-earth complexes, and organic ligands and semiconductor Nano particles with organic substituent's [7]-[8]. In the mean time, the red light-emitting materials have remained to be the weakest part in realizing the full color display. Low electroluminescence (EL) efficiency and impure EL spectrum due to the existence of visible light in NIR emission limit their practical application [7], [8].

II. EXPERIMENTAL

In this article we realized NIR OLEDs based on a new NIR organic dye as an emissive layer by thermal evaporation technique. Usual structures of OLEDs are based on multi-layer organic small molecules sandwiched between two electrodes. They are made by sublimation of organic molecules in vacuum. For a simple fabrication, a single-layer OLED is possible [5]. In a simple OLED structure, a light emitting layer which can be a photovoltaic (PV) device can be used as such a black layer [5]–[8]. When the PV device serves as a solar cell, the absorbed photons convert to electrical power for elongating the operation lifetime in a limited battery capacity [6]. It can also function as the ambient light sensor to adjust the luminance level of a display for achieving suitable CR at different ambient Intensities [5] from the lowest unoccupied orbital's (LUMO)to the highest occupied molecular orbital (HOMO), produces photons with energy equal to the LUMO and HOMO difference. The released photons pass through the transparent electrode.

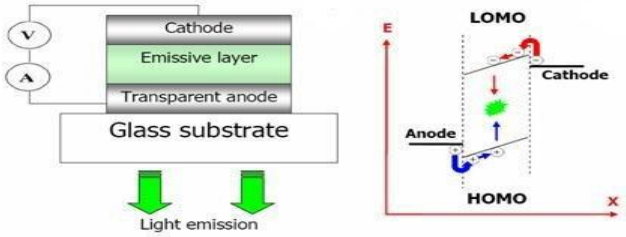

Fig. 1. Strucure of single layer OLED and Cathode will be Mg and transparent anode is ITO

As shown in Fig 1. Application of a forward bias at the diode terminals causes carrier injection through the organic layers from the electrodes. These carriers move toward each other in the emissive layer. A new red emission material, (E)-N-((E)-3-((E)-(4-iodo-phe nyl-imino) methyl) benzyl dine) -4-iodobenzenamine, was synthesized. Chemical structure and Absorption spectrum of this organic dye molecule shown is in Fig 2.

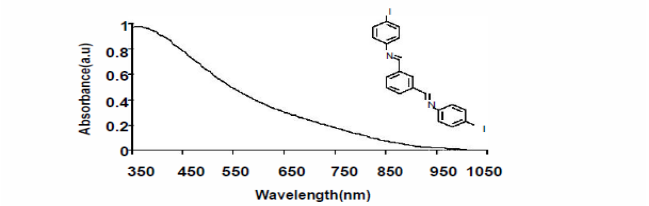

Fig. 2. Absorption spectrum and molecular structure of the dye used

Manuscript Received on January 2015.

Mr. Vijendra V, is a Student at Department of VLSI Design and Embedded Systems, Center for Post Graduate Studies, Visvesvaraya Technological University, Belagavi 590018, Karnataka, India.

Published By:
Blue Eyes Intelligence Engineering
& Sciences Publication

A new red emission material, (E)-N -((E)-3-((E)-(4-iodophe nyl-imino) methyl) benzyl dine) -4-iodobenzenamine, was synthesized. Chemical structure and Absorption spectrum of this organic dye molecule shown is in Fig 2. Circular devices with 2 mm diameter were made on 2cm x 2cm ITO slides. The active area of each device was 7.1 mm^2. OLEDs are fabricated on a glass substrate pre-coated with indium tin oxide (ITO) with a sheet resistance of 20 Ω/□ and a thickness of about 100 nm. Its work function is about 3.68 eV. The ITO substrate is washed and cleaned using acetone, ethanol and distilled water respectively.

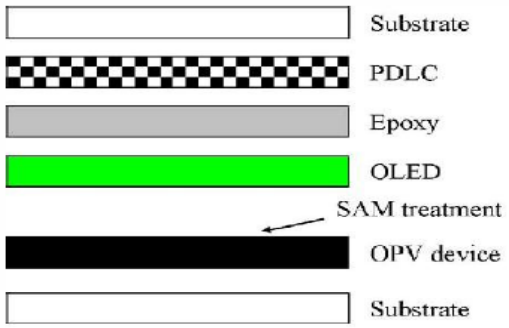

Fig. 3. Device configuration of the stack device (OPV/ OLED/ PLDC).

The OLED and OPV devices requires 100 nm Ag cathode, respectively. A passivation layer with UV resin was needed to prevent the OLED and OPV from the attack of the LC material. Due to the black background of OPV in our device, here, a polymer dispersed liquid crystal (PDLC) was selected for the RLCD mode in our tandem device, which exhibited the advantages of polarizer-free and wide viewing angle. Besides, no alignment layer was needed in our PDLC. Electrical properties (– characteristics) of OLED and OPV device were nearly the same in the OPV/ OLED and OPV/ OLED /LCD devices, which showed that the effectiveness of the passivation layer upon the OLED. Besides, such a configuration (passivation +LC between two glass substrate) successfully prevented the oxygen and water at-tacking the OLED and OPV device, which elongate the storage lifetime of these two devices. However, due to the insertion of the passivation layer, the driving voltage (T at 50%) under LC-mode operation increases from 15.1 to 34.5

III. EXCREMENTAL SETUP AND RESULTS

The device was fabricated on a patterned indium-tin- oxide (ITO) glass substrate, as shown in Fig. 4(a). After oxygen treatment for cleaning the substrate surface and increasing work function of ITO, poly(3,4-ethylenedioxythiophene): poly(styre- nesulfonate) (PEDOT:PSS) was spun onto the substrate (4000 rpm for 30 sec) followed by the baking process at the temperature of 150 C for 10 mins with the thickness of 20 nm. The pattern of PEDOT: PSS was formed by mechanical wiping with DI water. Then, poly(3-hexylthiophene): methanofullerene(PHT=108) dissolved in toluene was spun (700 rpm and 30 sec) and baked (slow dried for 45 min followed by150 C for 10 min) with the thickness of 220 nm. CHCl was used to wipe the edge of the device to define the pattern of P3HT:PCBM. PEDOT:PSS and P3HT:PCBM formed the organic layers of OPV, as shown in Fig. 4(b). Then, Ca and Ag were thermally deposited through shadow mask with the thickness of 20 and 12.5 nm, respectively to form the semi- transparent electrode (OPV cathode), as shown in Fig. 4(c) [2]. Ag thickness connecting OPV and OLED must be engineered. Thin and thick film resulted in bad conductivity and low transmission, respectively, which will be discussed in the next section. The overlapping region between the ITO anode, OPV layers, and Ca/Ag cathode defined the device area (2 mm x 2 mm). The semitransparent Ca/Ag also served as the anode of the OLED. To increase the work-function of Ag surface, we used the SAM with the mixture of n-decanethiol (HDT).

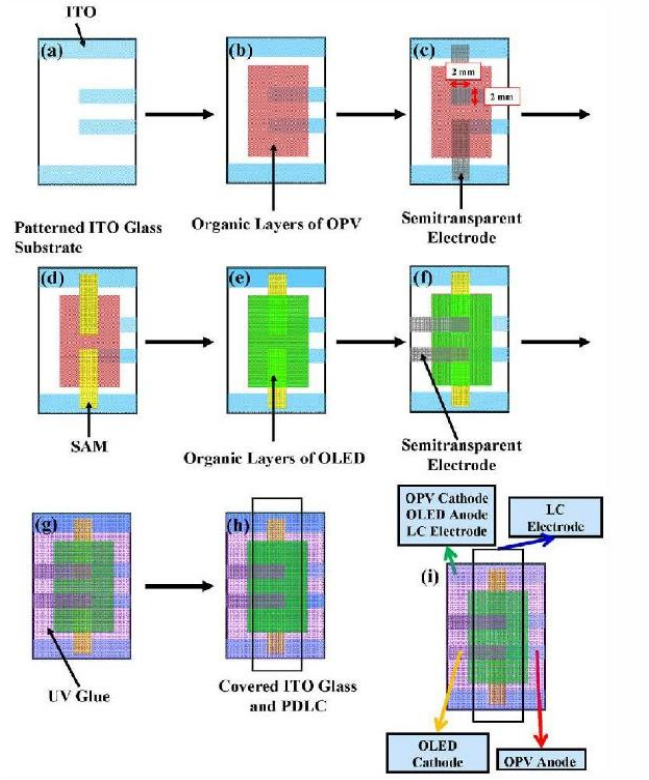

Fig. 4. Process flow for stacked device

heptadecafluoro-l-decanethiol(FDT)(HDTFDT) by stamping process. Patterned polydimethyl-siloxane (PDMS) mold was first immersed in SAM solution for 10 sec, and then stamped on the Ag surface inside the glove box, which effectively improved the work function from 4.7 to 5.3 eV and was suitable for OLED anode [2], as shown in Fig 4(d). Then, organic layers of OLED was then thermally deposited through shadow mask, with the stacks of N,N-Bis (naphthalen-1-yl)-N-N-bis(phenyl)benzidine (NPB) and tris-(8- hydroxyquinoline) aluminum (Alq), respectively, as the hole-transporting layer and electron-transporting layer (and emitting layer as well), with the thickness both at 60 nm, as shown in Fig 4(e) Then, similarly, Ca (20 nm) and Ag (12.5 nm) were thermally deposited through shadow mask to form the OLED cathode, as shown in Fig. 4(f), to complete the OLED process Another 100-nm NPB layer was deposited upon Ca/Ag to increase transmittance of the semitransparent electrode and stability of the OLED [4].

Published By:
Blue Eyes Intelligence Engineering
& Sciences Publication

Before the following LCD process, we spun on a UV-curable epoxy at 3000 rpm (HC8903E- Cyberbond), followed by UV curing process for 15 s to form a passivation layer with a thickness ~3 to 4/m to prevent the OPV and OLED from the attack of LC materials, Fig. 4(g) [3]. Another cover glass was used for the LCD fabrication (and encapsulation of OLED and OPV). The cell gap between two glass substrate was controlled at 8 micro meters by spacer powder with sides sealed by UV curable epoxy. Two small openings were left for LC material (E7NOA65=7:3)

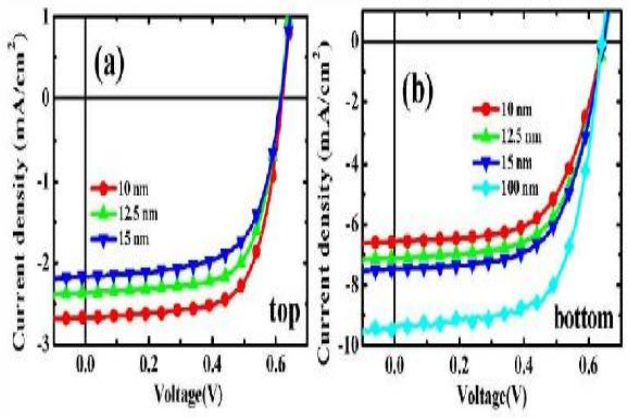

Fig. 5. $J-V$ characteristics of OPV -mode operation with different Ag cathode thicknesses under illumination from (a) top and (b) bottom, respectively, on the ITO-coated glass substrate.

Injection, and then sealed completely. Then, U V was applied again (10 mW /cm2 for 8 mins) which resulted in phase separation of PDLC via polymerization Fig. 4(h). Note that all the processes were done in a vacuum chamber and a glove box (with water and oxygen less than 1 ppm), which were connected by a transfer chamber. Our device experienced UV exposure for curing epoxy (15 s) and PDLC polymerization (8 mins) during fabrication, which may degraded the device performances of OLED and OPV underneath. To clarify the issue, we fabricated the integrated device and illuminated with UV light for 1 h, which showed little effect on electrical properties. There were some differences in optical characteristics due to thin film absorption and interference effect, as described later. That meant there was little material degradation of our OLED and OPV under UV light exposure, possible due to: (1) low power density of UV light; (2) good environment control inside glove box; and (3) stable fabrication techniques. We also fabricated some control devices to compare with fully tandem device (OPV/ OLED/ PDLC), such as OPV, OLED, PDLC, OPV/ OLED, OPV/ PD LC, and OLED/ PDLC. Typically, we started from ITO patterned glass substrate except specified. For driving and measuring the electrical characteristics of OLED and OPV, Keithley 2400 source meter was used. A spectrometer, Minolta CS-1000, was used for obtaining the luminance and electroluminescence spectra of OLED. Class A solar simulator provided the AM 1.5G 1-sun radiation on the OPV device. For $V-T$ characteristics of PDLC, a AC (1 kHz) electrical signal was provided through a function generator and a high-voltage amplifier. He–Ne laser (632.8 nm at 10 mW) was used as the light source and the optic al intensity was measured by Si-photo detector.

IV. RESULTS AND DISCUSSION

In our stacked device, one key layer is the semi transparent Ag used as cathodes of OPV (also the anode and cathode of OLED and the electrode of LCD) and OLED. At first, we studied electrical and optical effects of Ag-cathode thickness to individual OPV and OLED devices on the ITO -coated glass substrate, as shown in Figs. 5 and 6. Fig. 6(a) and (b) showed the $J-V$ characteristics of OPV with different Ag thickness when illuminating from bottom (glass substrate/ITO) and top (Ag) side, respectively, and Table I illustrated device performances. Because the light transmission decreased with increasing Ag thickness, we can see that short circuit current (J_{SC}) decreased when the Ag thickness increased from 10, 12.5, to 15 nm under top illumination

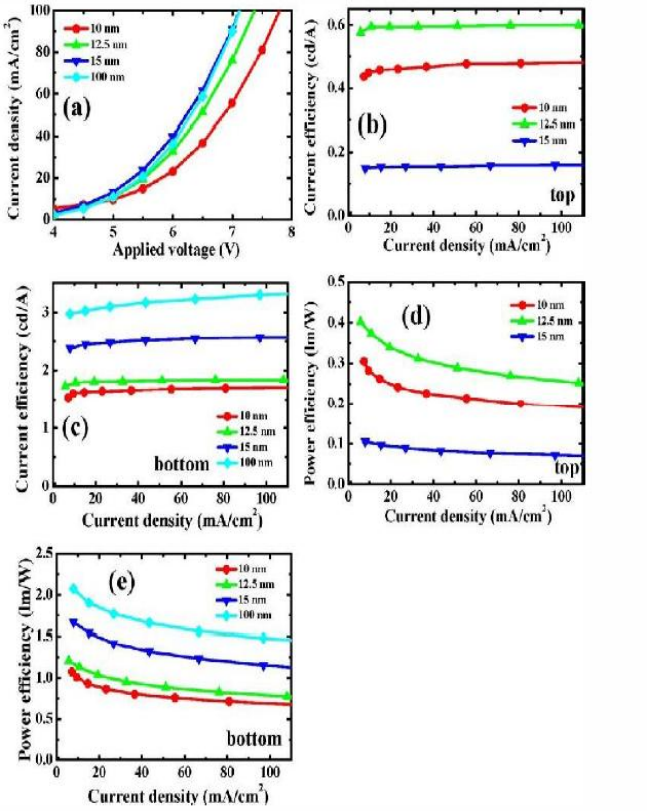

Fig. 6 (a) $J-V$ characteristics, (b) current efficiency (cd/A) versus J from top-emission, and (c) cd/A versus J from bottom-emission, (d) power efficiency (lm/W) versus J from top- emission, and (e) power efficiency (lm/W) versus J from bottom-emission of OLED-mode operation with different Ag cathode thicknesses, respectively, on the ITO-coated glass substrate.

On the other hand, J_{SC} increased with increasing the Ag thickness due to the stronger reflection from the Ag electrode. One can note that for the case with Ag =100 nm, J_{SC} can be measured only from the bottom side, because 100 nm Ag was measured only from the bottom side, because 100 nm Ag was opaque. One can also note that the J_{SC} ~2x_3x higher for bottom illumination case, compared with the top-illumination one, because: (1)

Published By:
Blue Eyes Intelligence Engineering
& Sciences Publication

ITO exhibited higher transmittance than Ag (ex: 80% and 38% for ITO and Ag=125 nm, respectively, at 550 nm) which resulted in higher absorption, and (2) micro-cavity effect coming from the semitransparent Ag for bottom illumination. One can also note that V_{OC} and fill factor (FF) values increased and decreased, respectively, for the bottom illumination cases, compared to the top illumination ones, which was also related to the increase of J_{SC}. Typically, J_{SC} and V_{OC} can be correlated by the following equation [4]:

$$V_{OC} \approx \frac{nk_BT}{q} \ln\left(\frac{J_{SC}}{J_S}\right)$$

where J_S and n is the reverse saturation current density of the device under dark condition and the i deal factor of the diode, respectively, k_B is Boltzmann's constant, J_S is reverse saturation currents, and T is the temperature. From (1), it was clearly seen that the increase of J_{SC} resulted in the increase of V_{OC}. Besides, under higher illumination (bottom illumination case in this study), the photo generated carriers experienced higher re-combination rate, which reduced the shunt resistance and FF [5].

TABLE I
DEVICE PERFORMANCES OF OPV MODE OPERATION EITH DIFFERENT AG CATHODE THICKNESS ON ITO COATED GLASS SUBSTRATE

Illumination from	Ag cathode thickness (nm)	V_{oc} (V)	J_{sc} (mA)	FF (%)	PCE (%)
Top	10	0.62	2.67	67.56	1.12
	12.5	0.62	2.36	66.92	0.98
	15	0.62	2.16	63.80	0.85
Bottom	10	0.65	6.57	60.11	2.57
	12.5	0.65	7.11	61.12	2.82
	15	0.65	7.48	61.44	2.98
	100	0.65	9.35	64.76	3.94

Fig. 6(a) showed the $J-V$ characteristics of OLED with different Ag-cathode thicknesses, and Table II illustrated device performances. We can see that there was 0.67 V increase at 100 mA $/$cm 2 for 10 nm Ag compared with control device (Ag =100 nm). When Ag =125 nm, the $J-V$ characteristics was close (0.24 V at 100 mA cm) and it was nearly identical when Ag =15nm. Fig. 4(b) and (c) showed the current efficiency (in terms of cd/A) at different current densities for different Ag thickness from bottom (glass substrate/ITO) and top-emission (Ag), respectively. Fig. 6(d) and (e) showed the power efficiency (in terms of lm/W) of devices corresponding to Fig. 6(b) and (c). OLED with 12.5 nm Ag as the cathode showed highest efficiency from top-emission compared to devices with 10 and 15 nm Ag, due to micro cavity effect. Typically, OLED can be viewed as a Fabry–Pérot cavity, which can be modeled as the product of wide angle and multi-beam interference [6]. The former one described the interference between the light leaving toward the viewing direction and the light reflecting back from the other direction, which was mostly decided by the distance from the emission dipoles to the back surface (ITO/glass interface at bottom side in this case). The multi-beam interference meant the interference travelling back and forth inside the micro cavity and determined by the total thickness and phase shift of the micro cavity. We have fabricated the Ag thin film (10, 12.5, and 15 nm) on the glass substrate and measured the transmittance and reflectance spectra (not shown here). For Ag=10125 and 15 nm, the transmittances. Values at 550 nm were 41%, 38%, and 31%, respectively. And the reflectance values at 550 nm were 19%, 42%, and 57%, respectively. Note that when Ag =10 and 15 nm, transmittance values were close (41% versus 38%) while there was a big difference between reflectance values (19% and 42%), which came from the enhanced plasmonic absorption of island growth of thin Ag films (10 nm) [4]. Considering the wide angle interference, the transmittance value for Ag =10 and 125 nm of the OLED cathode were close (41% and 38%, respectively) which resulted in similar effect. On the other hand, the in-creased reflectance of Ag =125 nm enhanced the multi-beam Interference effect and contributed to higher current efficiency. When further increasing Ag to 15 nm, the transmission was much lower and the reflection was much higher which yielded a much lower efficiency, compared to the cases with Ag=10 and 12.5 nm. For bottom emission, current efficiency increased monotonically with increasing Ag thickness, due to the increase of Ag reflection. Higher efficiency (listed in Table II) from bottom emission, compared to top one in the same device also proved the higher reflection and absorption of the Ag cathode, compared to the ITO anode with high transmittance. From the experimental results shown above, the Ag thickness in our OPV and OLED devices was chosen as 12.5 nm to achieve sufficient electrical conductivity and optical transmittance.

TABLE II
DEVICE PERFORMANCES OF OLED MODE OPERATION WITH DIFFERENT AG CATHODE THICKNESS, ON A ITO-COATED GLASS SUBSTRATE

Emission from	Ag cathode thickness (nm)	V	*Current efficiency (cd/A)	*Power efficiency (lm/W)
Top	10	7.79	0.47	0.19
	12.5	7.36	0.59	0.26
	15	7.13	0.16	0.07
Bottom	10	7.79	1.69	0.68
	12.5	7.36	1.86	0.78
	15	7.13	2.57	1.14
	100	7.12	3.31	1.49

*Measured at 100mA/cm2

Published By:
Blue Eyes Intelligence Engineering
& Sciences Publication

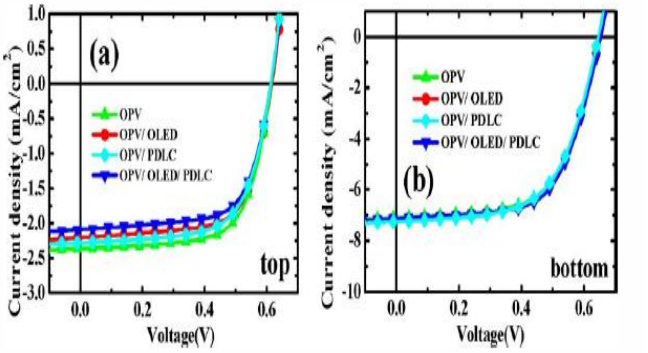

Fig. 7.1 $J-V$ characteristics of OPV-mode operation in an individual device and tandem devices (OPV/ OLED, OPV/ PDLC, and OPV/ OLED/ PDLC) under illumination from (a) top and (b) bottom, respectively.

TABLE III

DEVICE PERFORMANCES OF OPV-MODE OPERATION IN AN INDIVIDUAL DEVICE AND TANDEM DEVICES

Illumination from	Device	V_{oc} (V)	J_{sc} (mA)	FF (%)	PCE (%)
Top	OPV	0.62	2.36	66.92	0.98
	OPV+OLED	0.62	2.21	66.91	0.92
	OPV+PDLC	0.62	2.28	64.86	0.92
	OPV+OLED+PDLC	0.62	2.09	66.31	0.86
Bottom	OPV	0.65	7.11	61.12	2.82
	OPV+OLED	0.65	7.14	61.17	2.84
	OPV+PDLC	0.65	7.25	60.04	2.83
	OPV+OLED+PDLC	0.65	7.14	61.76	2.86

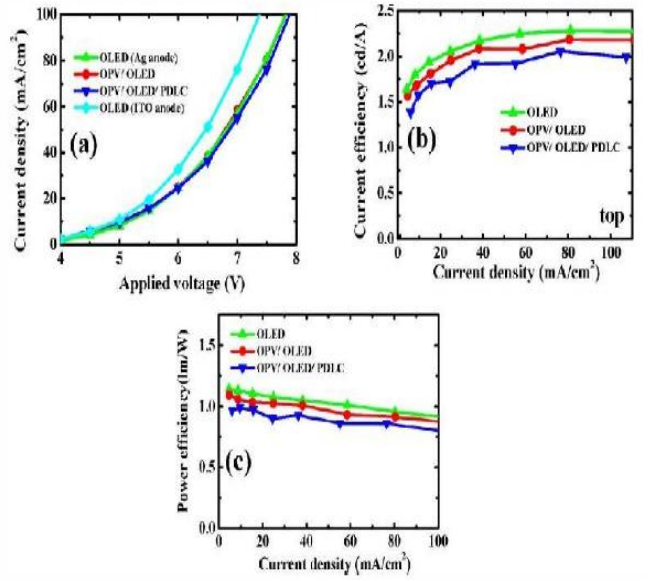

Fig. 7.2 (a) and (b) showed the $J-V$ characteristics of OPV device under top - and bottom-illumination, respectively, for the devices of OPV, OPV/ OLED, OPV/ PDLC, and OPV/ OLED/ PDLC. And Table III illustrated device performances.

Note that the PDLC was biased at 70 V, kept at transparent state, during the electrical and optical measurements of OPV and OLED.

TABLE IV

DEVICE PERFORMANCES OF OLED MODE OPERATION IN AN INDIVIDUAL DEVICE (OLED WITH AG AND ITO ANODE) AND TANDEM DEVICES (OPV/OLED AND OPV/OLED/PLDC)

Device	V	*Current efficiency (cd/A)	*Power efficiency (lm/W)
OLED (thin Ag anode)	7.81	2.28	0.91
OPV+OLED	7.80	2.17	0.88
OPV+OLED+PDLC	7.89	2.01	0.80
**OLED (ITO anode)	7.36	0.59	0.26

*Measured at 100 mA/cm².
**This device is the same as "Ag cathode thickness = 12.5 nm" in Table II and Fig. 4.

(Figs. 7 and 8) When light comes from the bottom side (ITO), there was little shift in $J-V$ characteristics in these four cases, which meant the electrical properties of OPV device was not affected by the SAM, OLED, and PDLC processes. However, one can note that J_{SC} decreased when OLED, PDLC, and OLED/ PDLC staked upon the OPV device, which came from the optical effect. For example, about 4% decrease at 550 nm in transmittance of passivation layer (UV resin) was observed, which accounted for the decrease in J_{SC} with introducing PDLC upon OPV. Optimization of micro cavity structure of OLED may be helpful for enhancing the transmittance and boosting up the OPV efficiency. Fig . 8(a) and (b) showed the $J-V$ and cd/A-J characteristics of OLED, respectively, for the devices of OLED, OPV/ OLED, and OPV/ OLED/ PDLC. And Table IV illustrated device performances. Note that in the tandem device, the anode of OLED was replaced from ITO to thin Ag, and it resulted in a slightly increase of driving voltage (0.4 V in 100 mA $/cm^2$), as shown in Fig. 7(a) besides, there was no obvious shift in $J-V$ characteristics in the tandem devices (OPV/ OLED and OPV/ OLED/ LCD). Under OLED operation, the bottom emission will be strongly absorbed by the OPV device. Hence we only focused on emission from the top side, as shown in Fig. 7(b) and (c)

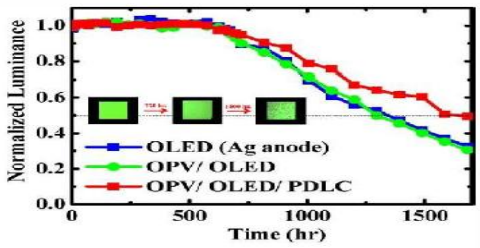

Fig. 8. Luminance of OLED measured at different time for OLED, OPV/ OLED, and OPV/ OLED/ PDLC. Inset shows the photos of lit-on OLED at different time.

Published By:
Blue Eyes Intelligence Engineering
& Sciences Publication

As anode and cathode layer, respectively, which corresponded to the curve, denoted by "12.5 nm" in Fig. 6(b) and Table II. Other devices in Table IV used thin Ag (12.5 nm) as both the anode and cathode for the OLED. In Table IV, comparing the two OLED devices (Ag and ITO anode), both with Ag cathode, one can see that Ag -anode OLED exhibited a higher in efficiency than ITO-anode one (2.28 and 0.59 cd/A, respectively). For the bottom emission OLED, the last row in Table II, the current efficiency was about 3.31 cd/A. As shown in [3], when using a thick Ag as the anode, and thin Ag as the cathode, the current efficiency boosted up to 10 cd /A. When reducing the thickness of Ag anode (as shown in the first row of Table IV), the reflectivity from anode side decreases, and hence the light emission from top-side decreased to 2.28 cd/A. Compared to the device with ITO anode and Ag thin cathode, one can see that light emission from top side is much higher for thin Ag anode, which was due to the enhanced multi-beam interference. Besides, in our organic material system, hole mobility of NPB was much higher than electron mobility of Alq3 [7]. Retardation of hole mobility with Ag anode resulted in more balanced carriers which may possibly another reason to explain the high efficiency from top-emission of devices with Ag-anode (the first three rows in Table IV), compared to ones with ITO-anode (in Table IV) [8]. Compared with an individual OLED, we can see that the efficiency (cd/A) decreased (by 4.8%) in OPV/ OLED device because of the absorption of OPV. Although OPV was placed underneath, however, the OPV absorbed some light which may reflect back to contribute to top- emission under OLED operation [29]. Besides, further 7.4% decrease in current efficiency was observed when stacking PDLC on OPV/ OLED, because of the reduction of transmission with the insertion of passivation layer. For an OLED and OPV device, a suitable encapsulation or passivation is needed because water and oxygen in ambient condition attacks such a device. With the increase of time, one can see the dark spot growth of OLED operation, as shown in the inset of Fig. 9 On the other hand, there is no easy method to observe such non-uniformity under OPV operation. Such OLED dark spots came from the loss of contact between electrode and organic materials underneath initialed from some defects [3]. In our integrated device (OPV/OLED) with OPV underneath the OLED, the ambient species (oxygen and moisture) would Attack the outmost metal (OLED cathode) first if the defects are only on the top-device (OLED). If the defects were on the substrate, it possibly attacks the OLED materials to the first (OLED cathode) and second Ag metal (OLED anode and OPV cathode) simultaneously.

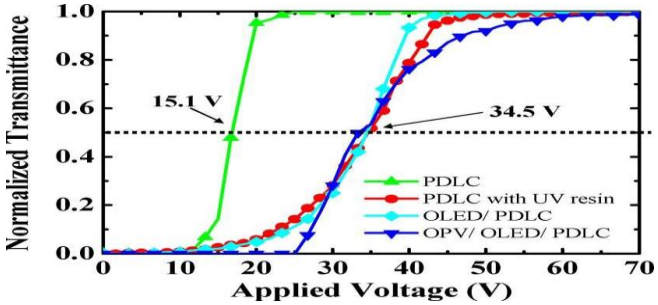

Fig. 9. V-T Characteristics of PDLC- mode operation in an individual device (PDLC and PDLC with UV resin) and tandem devices (OLED/ PDLC, and OPV/ OLED/ PDLC)

So we would see the failure region was close for OLED and OPV operation, if the non-uniformity of OPV operation in the integrated device was measurable, considering the metal-induced degradation. Besides, considering the degradation of OPV itself, it is also an merging research topic from material and devices [4]–[8] As shown in Fig. 7, we performed the storage lifetime test for our OLED operation in different devices. Here, we stored the devices under ambient condition and lit on the OLED every 24 hours with constant current density driving of 96 mA /cm 2 and measured the luminance for OLED, OPV/ OLED, and OPV/ OLED/ PDLC devices. One can see that stacking OPV and OLED did not affect the storage lifetime of OLED operation. It is reasonable because storage lifetime is determined by encapsulation process. Besides, when LC material was injected into the cavity between two glass substrate, it helped to repel the oxygen and water attacking OLED, and hence the operation lifetime increase. Note that we investigated the storage lifetime which was mainly affected by the ambient. Fig. 9 showed the V - T characteristics of PDLC operation in different devices. For an individual PDLC, 15.1 V was needed to achieve 50% of the normalized transmittance. However, with the insertion of UV resin on the top of the ITO, it resulted in a serious voltage drop and increased the voltage to 34.5 V. On the other hand, the thickness of OLED and OPV were quite thin (100–300 nm) which had little effect on driving voltage. An electrode on the top of passivation layer may solve this problem. But it may increase the complexity of the fabrication. One possible solution is to use the ultra-thin passivation layer (exhibiting suitable dielectric constant) upon the OLED, via the fabrication techniques such as atomic layer deposition (60 nm ZnO) or chemical vapor deposition (100 nm SiNx), to replace the thick epoxy layer ($\sim 34\mu m$ in thickness), and to reduce the driving -voltage [4], [5]. Other kinds of LCD mode (such as reversed -mode polymer stabilized cholesteric texture) or incorporation of nano-particle inside the LC matrix can be Employed to reduce the driving voltage as well [6], [7]. Be-sides, the total transmission of the whole device was degraded to 16.7%, due to the high reflection of thin Ag and the absorption of OPV. For display application, PDLC should operate as the reflective mode, which means a black (low reflection) back-ground is needed. Replacement of OPV anode to opaque anode, together with suitable micro cavity design of OPV and OLED will boost up the optical performances of OLED, OPV, and especially PDLC. Besides, in some cases (ex: PDLC device), use ITO rather than thin Ag as electrodes is an alternative to increase the contrast ratio.

V. CONCLUSION

The possibility to integrate OLED, OPV and LCD together with two glass substrate. Here, OPV was placed at the bottom acting as the black background and generating photon current. Thin (12.5 nm) Ag electrode was used to connect OPV and OLED, while SAM was applied on Ag to match the electrode work function. A passivation layer is applied on the top of OLED to avoid the attack of PDLC to OLED. In such a device, electrical properties of OLED and OPV are nearly identical to the individual device.

Published By:
Blue Eyes Intelligence Engineering
& Sciences Publication

Optical properties of OLED and OPV degrades a little and suitable cavity design will be needed. Storage lifetime of OLED-mode extended with PDLC insertion. Driving voltage of PDLC increases a lot, due to the insertion of passivation layer(3–4 μm) upon the PDLC electrode. A separate electrode on the top of the passivation will be needed to reduce the driving voltage. Use of thinner passivation layer and/or other LCD mode may be helpful as well. Replacing some electrodes from thin Ag to ITO may be helpful to the optical design for improving the optical characteristics (absorption of OPV, efficiency of OLED, and contrast ratio of PDLC). a new NIR dye has been synthesized for OLED applications. Single layer light-emitting diode has been fabricated by using a thermal evaporation technique. The device emitted a NIR light with a max at 800 nm. The turn-on voltages and the peak intensity in this OLED increased with thickness.

ACKNOWLEDGEMENT

Before we turn to publish this paper, I would like to add a few heartfelt words for the people who have been part of this publishing paper by supporting and encouraging me. At the onset, I would like to thank **almighty**. In particular, I would like to take this opportunity to express my Honor, Respect, Deepest Gratitude, and Genuine regards to my **Assitant Prof Mrs Amala M** for being a constant source of inspiration and motivation. I express my sincere thanks to the Faculty members ***Dept of VLSI Design & Embedded systems***, **Center for Post Graduate studies, Visvesvaraya Technological University, Belagavi** provided for the constant support and encouragement and Special thanks to Mr Zameer Ahamad B and Mr. Sateesh P Awari. I owe my special thanks to **My Parents** and my **Sister** for their moral support and warm wishes, and finally I would like to express appreciation to all **My Friends** for their support which helped me to complete this paper successfully.

REFERENCES

1. C. W. Tang and S. A. VanSlyke, “Organic electroluminescent diodes,” *Appl. Phys. Lett.*, vol. 51, no. 12, p. 913, 1987.
2. C. W. Tang, S. A. Vanslyke, and C. H. Chen, “Electroluminescence of doped organic thin films,” *J. Appl. Phys.*, vol. 65, p. 3610, 1989.
3. C. L. Lin, C. C. Hung, P. Y. Kuo, and M. H. Cheng, “New LTPS pixel circuit with AC driving method to reduce OLED degradation for 3D AMOLED displays,” *J. Display Technol.*, vol. 8, no. , pp. 681–683, 2012.
4. M. Yokoyama, C. M. Wu, and S. H. Su, “Enhancing the efficiency and contrast ratio of white organic light-emitting diode using energy-recy-clable photovoltaic cells,” *Jpn. J. Appl. Phys.*, vol. 51, p. 032102, 2012.
5. Y. H. Kim, S. Y. Lee, W. Song, M. Meng, Z. H. Lu, and W. Y. Kim, “High contrast green OLEDs using inorganic metal multilayer,” *Synth. Met.*, vol. 161, p. 2211, 2011.
6. S. Chen, J. Xie, Y. Yang, C. Chen, and W. Huang, “High-contrast top-emitting organic light-emitting diodes with a Ni/ZnS/CuPc/Ni con-trast-enhancing stack and a ZnS anti-reflection layer,” *J. Phys. D: Appl. Phys.*, vol. 43, p. 365101, 2010.
7. H. Cho and S. Yoo, “Polarizer-free, high-contrast inverted top-emitting organic light emitting diodes: Effect of the electrode structure,” *Opt. Express*, vol. 20, p. 1816, 2012.
8. T. L. Chiu, K. H. Chuang, C. F. Lin, Y. H. Ho, J. H. Lee, C. C. Chao, M. K. Leung, D. H. Wan, C. Y. Li, and H. L. Chen, “Low reflec-tion and photo-sensitive organic light-emitting device with perylene diimide and double-metal structure,” *Thin Solid Films*, vol. 517, no. 13, pp. 3712–3716, 2009
9. S. W. Liu, C. F. Lin, C. C. Lee,W. C. Su, C. T. Chen, and J. H. Lee, “High open-circuit voltage planar heterojunction organic photovoltaics exhibiting red electroluminescence,” *J. Electrochem. Soc.*, vol. 159, no. 2, p. H191, 2012.
10. C. J. Yang, T. Y. Cho, C.-L. Lin, and C. C. Wu, “Organic light-emitting devices integrated with solar cells: High contrast and energy recycling,” *Appl. Phys. Lett.*, vol. 90, no. 17, 2007.
11. T. Douseki, T. Yamada, J. Yamada, K. Ito, and K. Nishi, “Photovoltaic display module in a mobile GPS,” *Solar Energy Mater. Solar Cells*, vol. 67, p. 543, 2001.
12. T. Nakamura, H. Hayashi, M. Fuchi, M. Tada, T. Imai, H. Nakamura, K. Shigehiro, S. Hirota, S.Maruyama, A. Saitoh, and H. Kimura, “Display architecture suitable for multiple ambient light-sensor integration. using LTPS technology,” in *SID 08 Dig.*, 2008, pp. 720–723.
13. S. H. Kim, E. B. Kim, H. Y. Choi, D. H. Kang, W. H. Park, J. H. Oh, E. Y. Lee, S. H. Lee, D. H. Oh, K. H. Kim, M. H. Kang, J. H. Hur,J. Jang, J. W. Lee, J. R. Choi, S. H. Ahn, and S. W. Hong, “A 2 inch a-Si:H TFT-LCD with backlight control TFT sensors,” in *SID 07 Dig.*, 2007, pp. 1093–1096.
14. H. Hayashi, T. Nakamura, N. Tada, T. Imai,M. Yoshida, and H. Nakamura,“Optical sensor embedded input display usable under high-ambient- light conditions,” in *SID 07 Dig.*, 2007, pp. 1105–1108.
15. J. H. Lee, C. C. Liao, P. J. Hu, and Y. Chang, “High contrast ratio organic light-emitting devices based on CuPC as electron transport material,” *Synth. Met.*, vol. 144, p. 279, 2004.
16. S. T. Wu and D. K. Yang, *Reflective Liquid Crystal Displays*. New York, NY, USA: Wiley, 2001.
17. C. T. Wang and T. H. Lin, “Bistable reflective polarizer-free optical switch based on dye-doped cholesteric liquid crystal,” *Opt. Mater. Express*, vol. 1, p. 1457, 2011.
18. B.R.Yang, K. H. Liu, andH. P.D. Shieh, “Emi-flective display device with attribute of high glare-free-ambient-contrast-ratio,” *Jpn. J. Appl. Phys.*, vol. 46, p. 7418, 2007.
19. J. H. Lee, X. Zhu, Y. H. Lin, W. K. Choi, T. C. Lin, S. C. Hsu, H. Y. Lin, and S. T. Wu, “High ambient-contrast-ratio display using tandem reflective liquid crystal display and organic light-emitting device,” *Opt. Exp.*, vol. 13, no. 23, pp. 9431–9438, 2005.
20. H. M. Zhang, W. C. H. Choy, Y. F. Dai, and D. G. Ma, “The structural composite effect of Au-WO3-Al interconnecting electrode on performance of each unit in stacked OLEDs,” *Organ. Electron.*, vol. 10, pp. 402–407, 2009.
21. C. F. Lin, S. W. Liu, W. F. Hsu, M. Zhang, T. L. Chiu, Y. Wu, and J. H. Lee, “Modification of silver anode and cathode for top-illuminated organic photovoltaic device,” *J. Phys. D, Appl. Phys.*, vol. 43, no. 39, p. 395101, 2010.
22. C.C.Wu, C. F. Lin, J. H. Lee, W. F. Chang, T. L. Chiu, and S. W. Liu, “Fully Integration of Transflective Hybrid Device Consisting of PSCT and In-cell OLED,” in *SID 11 Dig.*, 2011, pp. 1602–1605.
23. C. F. Lin, S. W. Liu, C. C. Lee, J. C. Huang, W. C. Su, T. L. Chiu, C. T. Chen, and J. H. Lee, “Open-circuit voltage and efficiency improvement of subphthalocyanine-based organic photovoltaic device through deposition rate control,” *Sol. Energy Mater. Sol. Cells.*, vol. 103, p. 69, 2012
24. C.C.Wu, C. F. Lin, J. H. Lee, W. F. Chang, T. L. Chiu, and S. W. Liu, “Fully Integration of Transflective Hybrid Device Consisting of PSCT and In-cell OLED,” in *SID 11 Dig.*, 2011, pp. 1602–1605.
25. C. F. Lin, S. W. Liu, C. C. Lee, J. C. Huang, W. C. Su, T. L. Chiu, C.T. Chen, and J. H. Lee, “Open-circuit voltage and efficiency improvement of subphthalocyanine-based organic photovoltaic device through deposition rate control,” *Sol. Energy Mater. Sol. Cells.*, vol. 103, p. 69, 2012.
26. P. Schilinsky, C. Waldauf, J. Hauch, and C. J. Brabec, “Simulation of light intensity dependent current characteristics of polymer solar cells,”*J. Appl. Phys.*, vol. 95, p. 2816, 2004.
27. J. H. Lee, K. Y. Chen, C. C. Hsiao, H. C. Chen, C. H. Chang, Y.W.Kiang, and C. C. Yang, “Radiation simulations of top-emission organic light-emitting devices with two- and three-microcavity structures,” *J. Display Technol.*, vol. 2, no. 2, p. 130, Jun. 2006.
28. C. H. Hsiao, Y. H. Chen, T. C. Lin, C. C. Hsiao, and J. H. Lee, “Recombination zone in mixed-host organic light-emitting devices,” *Appl. Phys. Lett.*, vol. 89, p. 163511, 2006.

29. Z. D. Popovic and H. Aziz, “Reliability and degradation of small molecule-based organic light-emitting devices (OLEDs),” *IEEE J. Quantum. Electron.*, vol. 8, no. , p. 362, 2002.
30. H. C. Chen, J. H. Lee, C. C. Shiau, C. C. Yang, and Y.W. Kiang, “Electromagnetic modeling of organic light-emitting devices,” *J. Lightwave Technol.*, vol. 24, no. , p. 2450, 2006.
31. J. McElvain, H. Antoniadis, M. R. Hueschen, J. N. Miller, D. M. Roitman, J. R. Sheats, and R. L. Moon, “Formation and growth of black spots in organic light-emitting diodes,” *J. Appl. Phys.*, vol. 80, p. 6002, 1996.
32. C. D. Wang and W. C. H. Choy, “Efficient hole collection by introducing ultra-thin UV–ozone treated Au in polymer solar cells,” *Sol. Energy Mater. Sol. Cells*, vol. 95, p. 904, 2011.
33. Q. L. Song, M. L. Wang, E. G. Obbard, X. Y. Sun, X. M. Ding, X. Y. Hou, and C. M. Li, “Degradation of small-molecule organic solar cells,” *Appl. Phys. Lett.*, vol. 89, p. 251118, 2006.
34. S. W. Liu, C. C. Lee, C. F. Lin, J. C. Huang, C. T. Chen, and J. H. Lee, “Degradation of small-molecule organic solar cells,” *J. Mater. Chem.*, vol. 20, p. 7800, 2010.
35. C. Y. Chang and F. Y. Tsai, “Efficient and air-stable plastics-based polymer solar cells enabled by atomic layer deposition,” *J. Mater. Chem.*, vol. 21, p. 5710, 2011.
36. H. K. Kim, S. W. Kim, D. G. Kim, J. W. Kang, M. S. Kim, and W. J. Cho, “Thin film passivation of organic light emitting diodes by inductively coupled plasma chemical vapor deposition,” *Thin Solid Films*, vol. 515, p. 4758, 2007.
37. H. Ren and S. T. Wu, “Reflective reversed-mode polymer stabilized cholesteric texture light switches,” *J. Appl. Phys.*, vol. 92, p. 797, 2002.
38. Y. S. Ha, H. J. Kim, H. G. Park, and D. S. Seo, “Enhancement of electro-optic properties in liquid crystal devices.

AUTHORS PROFILE

Vijendra V, completed the B.E in Electronics and communication at C.Byregowda Institute of technology, Kolar, Karnataka and Pursuing Masters in VLSI Design and Embedded systems at Visvesvaraya technological university, Belagavi, Karnataka published one International and three National Conferences and Area of interest in the Quantum Mechanics, Solid state Physics, Digital Signal Processing, Bio-Medical Signals processing and Image Processing.